

Rich Tomography

Bill Lionheart, School of Mathematics, University of
Manchester and DTU Compute

July 2014

What do we mean by "Rich" Tomography?

- ▶ Conventional tomography reconstructs one scalar image from measurements of one scalar for each ray.
- ▶ In rich tomography make multiple measurements for each ray, and we aim to reconstruct a higher dimensional object, such as a vector, tensor or function, or exploit the redundancy in the data to reconstruct a scalar with fewer rays.
- ▶ Examples include
 - ▶ Spectral transmission tomography
 - ▶ Scattering tomography with energy sensitive detectors
 - ▶ Diffraction tomography
 - ▶ Polarized light tomography
 - ▶ Polarized neutron tomography
 - ▶ Doppler ultrasound tomography

Infrared spectral tomography

- ▶ Chemical species can be identified by their infra-red absorption spectra
- ▶ The spectra depend on temperature and pressure.
- ▶ By making measurements with multiple laser beams at multiple wavelengths one can attempt to image distribution of a chemical species or temperature
- ▶ This is used in industrial monitoring, and similar techniques used in atmospheric monitoring.
- ▶ While it is fairly easy to measure multiple wavelengths the number of rays measured is typically small.
- ▶ Typically this is treated as an absorption process and scattering is ignored. The opposite of Diffuse Optical Tomography.
- ▶ The misnomer 'hyperspectral' tomography/imaging is used, but this is for historical reasons as people had already used the word spectral imaging for just a few frequency. We will drop the 'hype'.

The experimental setup in [1]

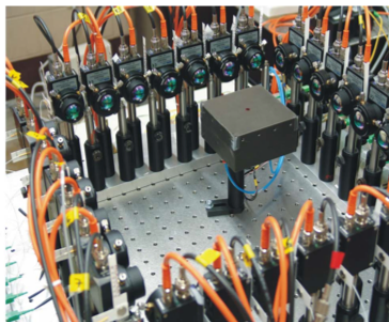
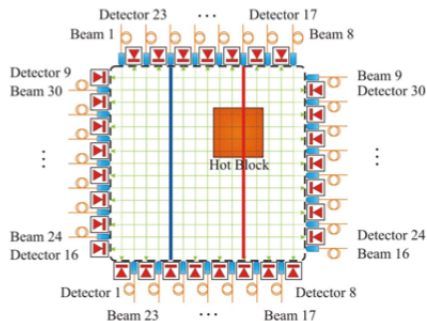


Fig. 1. (Color online) Optical beam/detector arrangement (left panel) and photograph (right panel) of the 15-by-15 sensor. This arrangement enables planar imaging in a 381 mm \times 381 mm (15 in. \times 15 in.) domain with 225 total pixels. Each intersection of laser beams (green in left panel) represents a pixel.

Spectral tomography in general

- ▶ $f(x)$ be the property we desire to image, $x \in \mathbb{R}^2$ the coordinate in the imaging plane.
- ▶ For each line $x_{p,\theta}(s) = p\theta^\perp + s\theta$ in the plane we assume we can measure the integral

$$Rf(p, \theta, \lambda) = \int \alpha(f(x_{p,\theta}(s)), \lambda) ds$$

for $\lambda_0 < \lambda < \lambda_1$.

- ▶ Here α is assumed monotonic as a function of x for λ in that range.
- ▶ Varying λ results in more data so can f be reconstructed with fewer projections than would be the case for conventional tomography?
- ▶ There are claims (Eg An et al) in the IRTT literature that two projections might be sufficient.

Simple discrete case

Consider the discrete case where f_{ij} is the pixel value on an $N \times N$ square x_{ij} .

We take only two projections in the coordinate directions at $\lambda = \lambda_k$, $k = 1 \dots K$ so that the data are

$$R_{1mk} = \sum_{j=1}^N \alpha(f_{mj}, \lambda_k), \quad R_{2mk} = \sum_{j=1}^N \alpha(f_{jm}, \lambda_k).$$

What we can deduce from just R_{1mk} where $m = 1 \dots N$ and $k = 1 \dots K = N$?

This is a system of N equations for N variables $(f_{mj})_{j=1}^N$.

Fixing a row of the image m the Jacobian matrix $(\partial R_{1mk} / \partial f_{mj})_{j,k=1}^N$ is invertible then the inverse function theorem guarantees that where a solution exists it is unique within a neighbourhood of that solution.

Note that

$$\partial R_{1mk} / \partial f_{ij} = \frac{\partial \alpha}{\partial f}(f_{mj}, \lambda_k)$$

so under fairly general conditions if the values of f_{mj} are different the columns of the Jacobian are independent vectors.

However R_{1mk} is invariant under permutation of the values in the vector $(f_{m,j})_{j=1}^N$.

Even if we can find the values of the pixels along that row, we have no hope of finding the order in which they occur from one projection. In general for given data R_{1mk} the solution $(f_{mj})_{j=1}^N$ will be unique up to a permutation $j \rightarrow \sigma(j)$ giving $N!$ solutions for that row.

For this one projection we can apply any permutation on any row of the image giving $N \cdot N!$ solutions.

The situation with two orthogonal projections is more complicated. Assuming we have been able to identify the values $\{f_{mj}\}_{j=1}^N$ for each m but not the ordering from one projection, and similarly $\{f_{jm}\}_{j=1}^N$ from the other projection, in the special case in which no value appears in two different rows the solution is unique. Of course in a practical problem we would have to interpret this as *sufficiently different* that we could tell them apart at the accuracy with which we measure.

By contrast an interesting case in which the solution for two projections is highly non-unique is the case where f_{ij} takes only N distinct values and these occur in each row and column. In this case R_{pmk} , $p = 1 \dots 2$ depends only on k . Any $N \times N$ Latin square where the values of the f_{ij} are the labels for the squares gives a solution. There are $L(N)$ $N \times N$ Latin squares where

$$\prod_{k=1}^N (k!)^{N/k} \geq L(N) \geq \frac{(N!)^{2N}}{N^{N^2}}$$

with for example $L(10)$ approximately 9.98×10^{36} .

More generally consider a subset M rows and M columns with $2 \leq M \leq N$ such there is a solution f_{ij} which has the Latin square property on the subset, that is there are M distinct values all appearing in each row and column. This subset can then be replaced by any of the $L(M)$ Latin squares. The simplest case is of course $M = 2$ and $L(2) = 2$ corresponding to swapping the values on the two diagonals. A fairly typical case in imaging might be that two values are quite common, for example a back ground level and a saturated or maximum level. Suppose that there are at least two regions that are saturated not in exactly the same rows and columns, then typically there will be a number Q of 2×2 subsets and 2^Q different solutions.

An et al's results

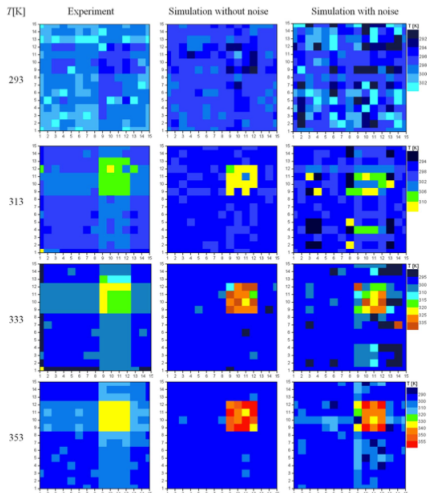


Fig. 5. (Color online) Four temperature reconstruction results for experimental data (first column), simulated noise-free data (second column), and simulated data with noise ($\sigma = 0.0002$, third column). Temperature at left indicates the temperature of the block. The ambient gas surrounding the block is at 297 K.

Scattering tomography

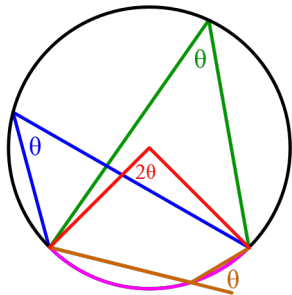
- ▶ For a certain range of energies of x-rays typical in security scanning and medical imaging inelastic Compton scattering is the most common scattering process.
- ▶ The wavelength of the photon changes from λ to λ' and it is scattered through an angle θ where

$$\lambda' - \lambda = K(1 - \cos \theta)$$

for a physical constant K

- ▶ Suppose we can supply x-rays at a known λ and measure the wavelength of the scattered x-rays.
- ▶ For a fixed source and receiver in the plane of a planar object the measurement is proportional to the electron density along the locus of points such that the rays to the source and detector meet at angle θ .

This is a circle by the Inscribed Angle Theorem



Cormack's inversion

Typically generalized (Funk)-Radon transform inversion of a function on the plane needs a two parameter family of curves. For example fix the source, move the detector along a line and measure at multiple scattered wavelengths.

This gives integrals over circles through a point (the source). Cormack [2] in a series of papers gave explicit inversion formulae for families of plane curves with polar (r, θ) form $\cos \sigma(\theta - \phi) = (p/r)^\sigma$. For $\sigma = 1$ this is fixed source, moving detector along a line and detecting all wavelengths (scattering angles).

Rigaud et al's description of Compton Scattering Tomography [5]

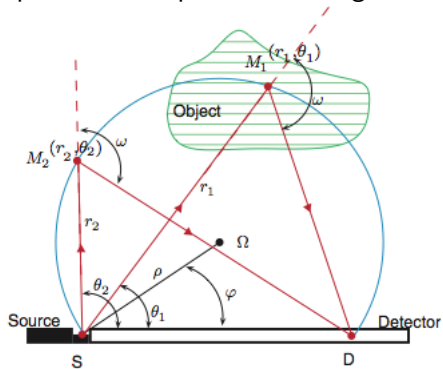


Figure 1. Principle of Norton's CST (CST₁).

$$r \cos(\theta - \phi) = 2\rho$$

There many generalizations see eg [3],[4].

Of course we can also vary over two space and one wavelength to give overdetermined data and solve numerically.

Perhaps we can use this to reduce errors from non-Compton scattering?

Back to Beer

Working at one energy in x-ray tomography we often forget that it is logarithm of the intensity that gives us a linear x-ray transform

$$\ln(I/I_0) = \int_{t=-\infty}^{\infty} -f(x + s\theta) ds$$

for a unit vector θ

This comes generally from a transport type equation (Beer Lambert Law)

$$\theta \cdot \nabla u(x, \theta) = -f(x)u(x, \theta)$$

which is really a first order hyperbolic PDE, which we integrate along characteristics,

$$I/I_0 = u(\infty)/u(-\infty) = \exp\left(\int_{s=-\infty}^{\infty} -f(x + s\theta) ds\right)$$

Typically measurements are integrated over various energies with *different* linear attenuation, so this is no longer linear.

What happens when u is some kind of vector or matrix?

Non abelian tomography!

Suppose u is a vector or matrix and f a matrix then as an ODE along rays one ray we have

$$\frac{d}{ds}u(s) = -f(s)u(s)$$

but for f non-scalar we do not generally have a solution $u(s) = \exp(-fs)u(0)$

While we can form the matrix exponential $\sum_{k=0}^{\infty} (-fs)^k/k!$ it does not satisfy $d \exp(-fs)/ds = -f \exp(-fs)$ unless f commutes with its derivative.

Polarized light tomography

In polarized light tomography u is the electric field along a ray and let f be (proportional to) the strain tensor then Rytov's law gives

$$\frac{d}{ds}u(s) = P_{\theta}(f(s))u(s)$$

where P_{θ} projects the matrix on to the subspace orthogonal to ray direction θ .

Novikov [6] shows that the inverse problem: 'find f from data from parallel beams and rotations about six axes' has a unique solution. Essentially his method uses Newton-Kantarovich method repeatedly updating using the solution of the linearized problem (line integrals of $P_{\theta}(f(s))$, the transverse ray transform).

A general non-abelian tomography

Eskin [7] considered a general non-abelian Radon transform in the plane of the form

$$\boldsymbol{\theta} \cdot \nabla u(x, \boldsymbol{\theta}) = (A_1(x)\theta_1 + A_2(x)\theta_2 + A_0(x)) u(x, \boldsymbol{\theta})$$

where u is a matrix function along each ray, and proved uniqueness of solution (up to a gauge condition) for the inverse problem of finding A_j from data along all rays. Proof uses complex analysis methods.

Note result is only in the plane (although the matrices are $n \times n$) and does not include Polarized light tomography (which is quadratic in $\boldsymbol{\theta}$)

Neutron spin tomography

In Neutron spin tomography we fire neutrons with a known spin direction through a material that has a spatially varying magnetic field and measure the spin state when it emerges.

For simplicity take the initial spin states to be each unit basis vector then assemble the resulting spin states along a ray as a 3×3 matrix u . The transport law is

$$\theta \cdot \nabla u(x, \theta) = M(B(x))u$$

where $B(x)$ is the magnetic field and $M(B)$ is proportional to skew symmetric matrix of the linear map $v \mapsto v \times B$, the vector product. Eskin's theorem then gives us $M(B(x))$ as his A_0 , at least for B smooth and from this we can deduce B .

Note that neutron spin tomography can be done a plane at a time so the planar result is enough.

References I

1. X. An et al, 2011, Validation of temperature imaging by H₂O absorption spectroscopy using hyperspectral tomography in controlled experiments, Applied Optics, 50, No 4
2. AM Cormack 1981 The Radon transform on a family of curves in the plane, Proc. Am. Math. Soc. 83, 32530 (and 1982, 86, 293-8)
3. TT Truong, and MK Nguyen, 2011, Radon transforms on generalized Cormacks curves and a new Compton scatter tomography modality, Inverse Problems, 27 , 12500
4. G Rigaud, 2013, On the inversion of the Radon transform on a generalized Cormack-type class of curves, Inverse Problems, 29, 115010
5. G Rigaud , MK Nguyen and AK Louis, 2012 Novel numerical inversions of two circular-arc radon transforms in Compton scattering tomography, Inverse Problems in Science and Engineering, 20:6, 809-839

References II

6. RG Novikov, 2009 On iterative reconstruction in the nonlinearized polarization tomography , Inverse Problems, 25, 115010
7. G Eskin, On the non-abelian Radon transform, 2004
arXiv:math/0403447, and Russ. J. Math. Phys. 11 (2004), no. 4, 391408.
8. M Dawson, et al, Imaging with polarized neutrons, 2009, New J. Phys. 11 043013